Journal of the American College of Cardiology Vol. 60, No. 12, 2012

Published by Elsevier Inc.
ISSN 0735-1097/$36.00
http://dx.doi.org/10.1016/j.jacc.2012.04.043

Longitudinal Left Ventricular Function for Prediction of Survival in Systemic Light-Chain Amyloidosis

Incremental Value Compared With Clinical and Biochemical Markers

Sebastian J. Buss, MD,* Mostafa Emami, BSc,* Derliz Mereles, MD,* Grigorios Korosoglou, MD,* Arnt V. Kristen, MD,* Andreas Voss, PhD,† Dieter Schellberg, PhD,‡§ Christian Zugck, MD,* Christian Galuschky, MS,‖ Evangelos Giannitsis, MD,* Ute Hegenbart, MD,¶ Anthony D. Ho, MD,¶ Hugo A. Katus, MD,* Stefan O. Schonland, MD,¶ Stefan E. Hardt, MD*

Heidelberg and Munich, Germany

Objectives The aim of the study was to determine whether longitudinal left ventricular (LV) function provides prognostic information in a large cohort of patients with systemic light-chain (AL) amyloidosis.

Background AL amyloidosis is associated with a high incidence of cardiovascular events. Reduced myocardial longitudinal function is one of the hallmarks of myocardial involvement in this rare disease.

Methods Two hundred six consecutive patients with biopsy-proven AL amyloidosis were investigated in this prospective observational study. Echocardiographic imaging parameters, mean tissue Doppler-derived longitudinal strain (LS), and two-dimensional global longitudinal strain (2D-GLS) of the LV, cardiac serological biomarkers, and comprehensive clinical disease characteristics were assessed. The primary endpoint was all-cause mortality or heart transplantation.

Results After a median follow-up of 1207 days, LS and 2D-GLS were significant predictors of survival in AL amyloidosis. The cutoff values discriminating survivors from nonsurvivors were −10.65% for LS and −11.78% for 2D-GLS. In a multivariable echocardiographic Cox model, only diastolic dysfunction and 2D-GLS remained as independent predictors of survival. In comprehensive clinical models, 2D-GLS ($p < 0.0001$), diastolic dysfunction ($p < 0.01$), the pathologic free light chains ($p < 0.05$), cardiac troponin-T (cTnT) ($p < 0.01$), and the Karnofsky index ($p < 0.001$) remained as independent predictors. 2D-GLS delineated a superior prognostic value compared with that derived from pathologic free light chains or cTnT in patients evaluated before firstline chemotherapy ($n = 113$; $p < 0.0001$), and remained the only independent predictor besides the Karnofsky index in subjects with preserved LV ejection fraction (≥50%; $n = 127$; $p < 0.01$). LS and 2D-GLS both offered significant incremental information ($p < 0.001$) for the assessment of outcome compared with clinical variables (age, Karnofsky index, and New York Heart Association functional class) and serological biomarkers.

Conclusions In the largest serial investigation reported so far, reduced LV longitudinal function served as an independent predictor of survival in AL amyloidosis and offered incremental information beyond standard clinical and serological parameters. (J Am Coll Cardiol 2012;60:1067–76) © 2012 by the American College of Cardiology Foundation

Amyloidosis is a multisystem disease with extracellular deposition of pathological insoluble beta-fibrillar proteins in a number of different organs, including the heart (1,2). Diagnosis and classification of amyloidosis is based on the analysis of the deposited insoluble abnormal fibrils (3,4). Involvement of the heart is seen in more than one-half of the patients with systemic light-chain (AL) amyloidosis. In this rare clonal plasma cell disorder, the extent and severity of cardiac involvement is the most important determinant of clinical outcome (1,5–7).

See page 1077

From the *Department of Cardiology, University of Heidelberg, Heidelberg, Germany; †Department of Psychology, University of Heidelberg, Heidelberg, Germany; ‡Department of Visceral and General Surgery, University of Heidelberg, Heidelberg, Germany; §Department of Psychosomatic and General Internal Medicine, University of Heidelberg, Heidelberg, Germany; ‖TomTec Imaging Systems GmbH, Munich, Germany; and the ¶Department of Hematology and Oncology, University of Heidelberg, Heidelberg, Germany. Dr. Buss received the "Wilhelm P. Winterstein" award from the German Heart Foundation for this work. Mr. Galuschky is an employee of TomTec Imaging Systems. Dr. Giannitsis has received financial support for clinical trials from Roche Diagnostics, Germany; is a consultant to Roche Diagnostics; and receives honoraria for lectures from Roche Diagnostics. Dr. Katus has developed the cTnT assay and holds a patent jointly with Roche Diagnostics; has received grants and research support from several companies; and has received honoraria for lectures from Roche Diagnostics. All other authors have reported that they have no relationships relevant to the contents of this paper to disclose. Drs. Schonland and Hardt contributed equally to this work.

Manuscript received January 29, 2012; revised manuscript received April 5, 2012, accepted April 10, 2012.

JACC Vol. 60, No. 12, 2012
September 18, 2012:1067–76

Abbreviations and Acronyms

2D-GLS = two-dimensional global longitudinal strain
AL = light-chain
cTnT = cardiac troponin-T
df = degree of freedom
E/e′ ratio = ratio of peak early diastolic mitral inflow velocity (E) to peak early diastolic mitral annular velocity (e′)
EF = ejection fraction
IDI = integrated discrimination improvement
LS = longitudinal strain
LV = left ventricular
MDRD = Modified Diet in Renal Diseases
NT-proBNP = N-terminal pro–B-type natriuretic peptide
NYHA = New York Heart Association
ROC = receiver-operating characteristic
TDI = tissue Doppler imaging

Cardiac biomarkers, such as cardiac troponin-T (cTnT) and natriuretic peptides, particularly N-terminal pro–B-type natriuretic peptide (NT-proBNP), play a central role for the assessment of prognosis in AL amyloidosis (8–10). Echocardiography is one of the main diagnostic tools used in patients with suspected cardiomyopathies, including cardiac involvement in AL amyloidosis (11,12). Non-Doppler–derived echocardiographic parameters like increased left ventricular (LV) wall thickness and decreased fractional shortening are independent predictors of cardiac mortality in AL amyloidosis (7). Previous studies elegantly demonstrated the usefulness of tissue Doppler and strain imaging (11,12) for diagnosis and staging of cardiac dysfunction in patients with AL amyloidosis (13–15). In addition, recent evidence found that tissue Doppler imaging (TDI)-derived myocardial systolic strain is associated with overall prognosis in AL amyloidosis (16,17), but the prognostic relevance of these parameters in relation to hematologic parameters and cardiac biomarkers has not been defined. Newer methods such as 2-dimensional strain echocardiography (11,12), which have previously been shown to have great clinical impact on other cardiovascular disorders (18,19), have so far not been investigated regarding prognosis in AL amyloidosis.

The purpose of this study was to clarify whether new noninvasive imaging techniques, such as TDI, TDI-derived strain imaging, and two-dimensional strain imaging provide further prognostic information in addition to serum biomarkers such as NT-proBNP and cTnT in a large cohort of patients with AL amyloidosis over a long follow-up period.

Methods

Setting and participants. Three hundred thirteen consecutive patients with suspected or known systemic AL amyloidosis were assessed at the interdisciplinary Heidelberg Amyloidosis Center and underwent evaluation of cardiac involvement in AL amyloidosis from July 2005 to October 2008. Patients with hereditary, AA, or senile amyloidosis (n = 51) or localized amyloidosis (n = 27) were excluded, as were patients with significant valvular heart disease, persistent atrial fibrillation, or inadequate performance on echocardiograms (n = 29). Thus, the final study population consisted of 206 consecutive patients (112 males and 94 females) with proven systemic AL amyloidosis. Diagnosis of AL amyloidosis was based on presence of a monoclonal gammopathy by serum electrophoresis, immunofixation on serum and urine, and free light chain test, and confirmed by positive Congo red staining with birefringence under polarized light of any biopsy (periumbilical fat aspiration, rectum, or target organ), positive immunohistology for kappa or lambda in the biopsy, and on the exclusion of hereditary forms of amyloidosis. The institutional review board approved the study conforming to the Declaration of Helsinki guidelines, and informed consent was obtained from all subjects. All clinical, echocardiographic, and laboratory test results were collected on the same day. A detailed description of the echocardiographic and laboratory methods is given in the Online Appendix.

Echocardiography. We performed a standard echocardiographic investigation with a commercially available ultrasound system (iE33, Philips Medical Systems), followed by two-dimensional color tissue Doppler recordings, for the offline assessment of tissue Doppler velocities and mean longitudinal strain (LS). The two-dimensional color tissue Doppler recordings with second harmonic imaging were collected during a brief breath hold, from the apical 4-, 2-, and 3-chamber views as previously described (Fig. 1A) (20). For offline 2-dimensional strain imaging (radial, circumferential, and longitudinal strain), the vendor independent offline 2D Cardiac Performance Analysis software (TomTec Imaging Systems, Munich, Germany) was used. For the assessment of global two-dimensional longitudinal strain (2D-GLS), we calculated the average of the longitudinal systolic peak negative values obtained from the 6 LV segments in the apical 4-, 2-, and 3-chamber views (Fig. 1B, Online Videos 1 and 2).

Outcomes and follow-up. All-cause mortality or heart transplantation due to progressive disease (n = 14) was the primary endpoint, because the classification of death is often problematic in AL amyloidosis. Follow-up was obtained by review of the patient's hospital chart or telephone interview with the patient or relative.

Statistical analysis. Data were analyzed using SPSS Version 19 (IBM Corporation) and MedCalc Version 11.5 (MedCalc Software, Belgium). Data were expressed as mean ± SD. Group differences for continuous variables were tested using the unpaired *t* test, for ordinal variables with the Mann-Whitney test, and differences between nominal variables were assessed using the Fisher exact test. Correlation analyses were performed using Spearman's coefficient. Kaplan-Meier curves were used to estimate the distribution of survival as a function of the follow-up duration. The association of clinical, echocardiographic, and serological parameters with outcome was investigated by multivariable Cox proportional-hazards regression models. In addition, integrated discrimination improvement analysis was performed using the same hierarchical model (21). Receiver-operating characteristics (ROCs) were used to estimate the value of echocardiographic and serological parameters to predict mortality. A subgroup analysis was

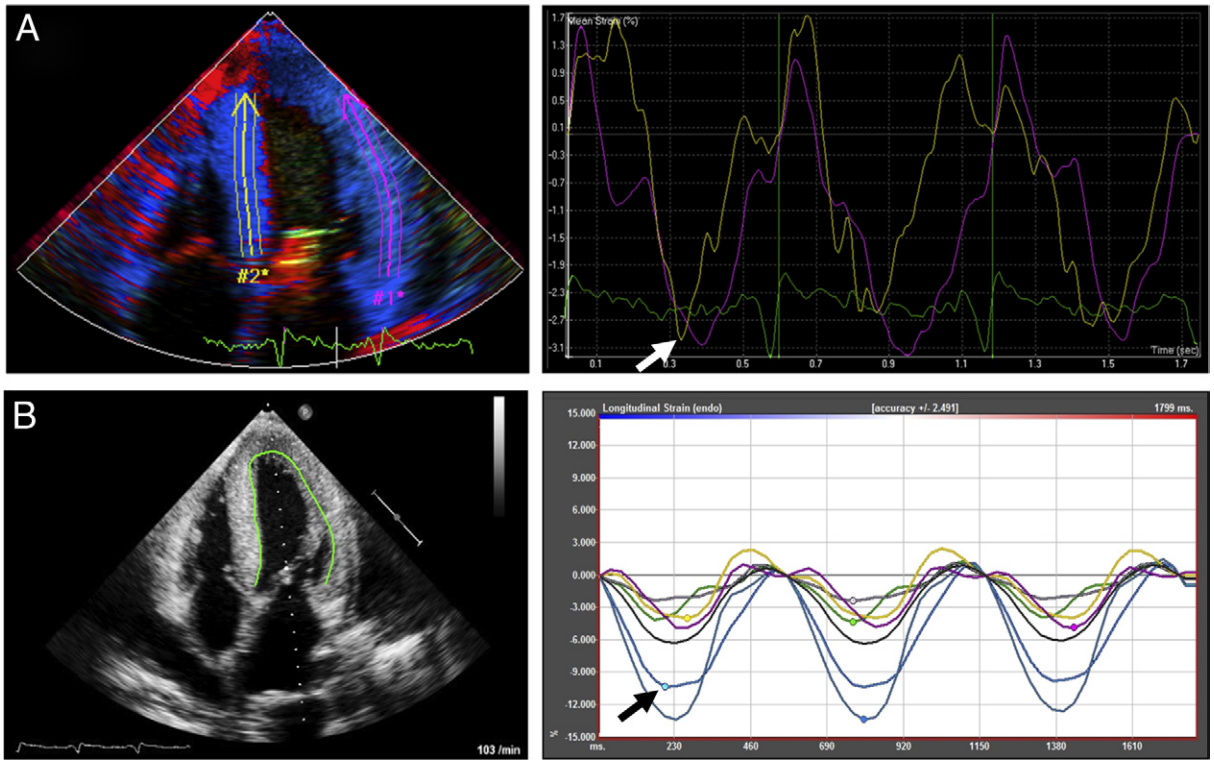

Figure 1 **Measurement of Left Ventricular Longitudinal Function**

Representative images illustrating the methods for measurement of tissue Doppler–derived mean longitudinal strain (LS) **(A)** and two-dimensional global longitudinal strain (2D-GLS) **(B)** in a patient with severe cardiac involvement in light-chain (AL) amyloidosis, who died 1 month after echocardiography. With both methods, LS is markedly reduced. In these examples, LS is calculated from the mean value of the peak negative strain values derived from the "M-Line" regions of interest **(white arrow in A)** or the mean peak negative strain **(black arrow in B)** of all 6 automatically segmented segments (**colored lines**; the **black line** represents the mean curve of all segments) in the apical 4-chamber view **(B)**. Apical regions cannot be evaluated with tissue Doppler due to the angle dependency of the method. For further illustration, see Online Video 1 (standard ultrasound examination) and Online Video 2 (assessment of GLS).

then performed by fitting the final multivariable model obtained in the overall analysis on the subgroup of patients who received echocardiography before firstline chemotherapy, with a preserved (≥50%) or reduced LV ejection fraction (EF) (<50%). Differences were considered statistically significant at $p < 0.05$. The authors had full access to the data and take responsibility for its integrity. All authors read and agreed to the paper as written.

Results

Characterization of study population. Two hundred six patients were included in the final analysis. One patient was lost at follow-up. The clinical characteristics as well as biomarkers are shown in Table 1. Standard two-dimensional echocardiographic parameters as well as the parameters for longitudinal function and strain imaging are illustrated in Table 2 and Online Table 1. Eighty-seven patients were treated with chemotherapy before study inclusion. Of those patients who had an echocardiogram before chemotherapy (n = 121), 37 (31%) received high-dose melphalan therapy, 62 (51%) received melphalan and dexamethasone, and 22 (18%) received other forms of therapy.

LV longitudinal function. LV longitudinal function can currently be assessed without vigorous effort in a clinical routine setting by the determination of LS and 2D-GLS. Both yielded a very good correlation with NT-proBNP, but a lower correlation for cTnT. The Spearman correlation of NT-proBNP with LS was $r = -0.79$ ($p < 0.001$), and with 2D-GLS, it was $r = -0.72$ ($p < 0.001$). In contrast for cTnT, the values for LS were $r = -0.65$ ($p < 0.001$) and $r = -0.62$ ($p < 0.001$) for 2D-GLS.

Survival analysis. Of the 205 patients, 109 (53%) died or received heart transplantation (n = 14) during follow-up. Deceased patients had significantly lower values for clinical, serological, and standard echocardiographic parameters as well as LV longitudinal function (Tables 1 and 2, Online Table 1). The median follow-up time after echocardiography was 1,207 days (255 days for nonsurvivors and 1,796 days for survivors). In the unadjusted univariate analysis (Table 3), clinical symptoms of congestive heart failure, cTnT, NT-proBNP, and parameters of myocardial morphology and function, assessed with echocardiography, were all significantly associated with overall survival. The measures for LV longitudinal function, LS, and 2D-GLS were

Table 1 Clinical Characteristics

Parameter	All Patients (n = 206)	Nonsurvivors (n = 109)	Survivors (n = 96)	p Value
Age (yrs)	60 ± 9	59 ± 9	61 ± 9	NS
Male (%)	112 (54)	64 (59)	48 (50)	NS
BMI (kg/m^2)	25 ± 4	24 ± 4	25 ± 4	NS
Heart rate (beats/min)	80 ± 15	82 ± 16	78 ± 14	<0.05
Systolic blood pressure (mm Hg)	112 ± 23	104 ± 23	121 ± 20	<0.0001
Diastolic blood pressure (mm Hg)	74 ± 12	70 ± 13	79 ± 9	<0.0001
NYHA functional class	2 (1; 3)[a]	3 (2; 3)[a]	1 (0; 2)[a]	<0.0001
No. of amyloid organs involved	2.7 ± 1	2.8 ± 1.1	2.6 ± 1.1	NS
MDRD (ml/min/1.73 m^2)*	60 ± 32	56 ± 32	65 ± 33	NS
Subjects with dialysis (%)	18 (9)	10 (9)	8 (8)	NS
ECG low voltage present (%)	49 (24)	33 (30)	16 (17)	<0.01
NT-proBNP (pg/ml)	2,579 (300; 6,871)†[a]	5,214 (2,454; 12,112)†	430 (153; 2,147)†	<0.0001
cTnT (μg/l)	0.020 (0.005; 0.100)†	0.050 (0.020; 0.180)†	0.005 (0.005; 0.020)†	<0.0001
Mayo score‡	2 (2; 3)	3 (2; 3)†	2 (1; 2)†	<0.0001
Free light chain difference§ (mg/l)	343 ± 738	546 ± 946	106 ± 222	<0.0001
Karnofsky index‖ (%)	77 ± 9	73 ± 8	81 ± 7	<0.0001

Values are mean ± SD or n (%). p Values are listed for survivors versus nonsurvivors. *Glomerular filtration rate estimated with the Modified Diet in Renal Diseases (MDRD) formula. †Median (quartile 1; quartile 3). ‡Mayo cardiac biomarker staging score (8). §Difference between pathologic and nonpathologic serologic free light chains. ‖Karnofsky performance status scale.
BMI = body mass index; cTnT = cardiac troponin-T; ECG = electrocardiography; NT-proBNP = N-terminal pro–B-type natriuretic peptide; NYHA = New York Heart Association.

clearly associated with a reduced survival in patients with AL amyloidosis (Fig. 2).

Proportional hazards models. Different echocardiographic parameters that were previously attributed to be prognostic in AL amyloidosis were further investigated for their predictive value in all patients. First, in a stepwise Cox regression analysis of relevant echocardiographic values (including all strain variables) only 2D-GLS ($p < 0.001$) and the ratio of peak early diastolic mitral inflow velocity (E) to peak early diastolic mitral annular velocity (e′) (E/e′ ratio) ($p < 0.01$) remained as independent predictors for survival. A representative multivariate model that covers several established echocardiographic parameters is shown in Table 4. These results confirmed that global LV longitudinal function represented by 2D-GLS (hazard ratio [HR]: 0.82, $p < 0.0001$) was an independent echocardiographic predictor of survival along with a weak effect of diastolic dysfunction represented by the E/e′ ratio (HR: 1.02, $p = 0.035$; Table 4).

For the final multivariate comprehensive clinical models (n = 198), which included well-recognized cardiac and other risk factors for AL amyloidosis, we therefore chose 2D-GLS and the E/e′ ratio as echocardiographic variables (Table 5). In 5 patients, New York Heart Association (NYHA) class was not available due to muscular disorders because of polyneuropathy, and in 2 patients, serologic free light chains values were missing. The model revealed the Karnofsky index (HR: 0.94, $p = 0.0002$), the free light chain difference (HR: 1.0002, $p = 0.047$), cTnT (HR: 1.97, $p = 0.007$), E/e′ ratio (HR: 1.03, $p = 0.011$), and 2D-GLS (HR: 0.85, $p < 0.0001$) as the only significant independent predictors of survival.

Table 2 Echocardiographic Characteristics

Parameter	All Patients (n = 206)	Nonsurvivors (n = 109)	Survivors (n = 96)	p Value
Left atrial volume index (ml/m^2)	33.9 ± 14	37.0 ± 13.5	30.5 ± 13.9	<0.001
Septal wall thickness (mm)	15.2 ± 3.6	16.7 ± 3.7	13.4 ± 2.7	<0.001
LV mass index (g/m^2)	138.8 ± 45.5	156.4 ± 48.0	119.2 ± 33.2	<0.0001
Ejection fraction (%)	51.7 ± 11.5	47.3 ± 12.1	56.5 ± 8.6	<0.001
E/e′ ratio	15.3 ± 9.7	19.7 ± 10.5	10.4 ± 5.5	<0.0001
Pericardial effusion present (%)	92 (45)	64 (59)	27 (28)	<0.0001
Mitral annular plane systolic excursion (cm)	1.1 ± 0.5	0.8 ± 0.4	1.4 ± 0.4	<0.0001
Tissue Doppler				
Peak systolic mitral annular velocity (s) (cm/s)	7.0 ± 2.6	5.8 ± 2.3	8.4 ± 2.2	<0.0001
Mean LS systolic (%)	−10.4 ± 5.7	−7.2 ± 4.4	−14.0 ± 4.8	<0.0001
2-dimensional				
Mean 2D-radial peak positive strain (%)	27.8 ± 9.9	26.2 ± 9.6	29.7 ± 9.8	<0.01
Mean 2D-circumferential peak negative strain (%)	−21.4 ± 6.0	−20.0 ± 5.7	−23.1 ± 6.0	<0.001
2D-GLS (%)	−13.1 ± 5.4	−9.8 ± 4.4	−16.7 ± 3.8	<0.0001

Values are mean ± SD or %. p Values are listed for survivors versus nonsurvivors.
E/e′ ratio = ratio of peak early diastolic mitral inflow velocity (E) to peak early diastolic mitral annular velocity (e′); LS = longitudinal strain; 2D-GLS = two-dimensional global longitudinal strain.

Table 3 Univariate Analysis for Overall Survival

Variable	HR	95% CI	p Value (Unadjusted)
Age (yrs)	1.00	0.9902–1.0323	0.303
NYHA functional class (≥2)*	4.23	2.846–6.289	<0.0001
Karnofsky index (%)	0.91	0.8876–0.9272	<0.0001
MDRD† (ml/min/1.73 m^2)	0.99	0.9884–1.0000	0.053
Free light chain difference‡ (mg/dl)	1.00	1.0009–1.0014	<0.0001
cTnT (>0.03 μg/l)*	4.95	3.3308–7.3418	<0.0001
Log NT-proBNP (pg/ml)	2.94	2.3473–3.6874	<0.0001
ECG low voltage present*	1.78	1.1797–2.6713	<0.01
Left atrial volume index (ml/m^2)	1.03	1.0140–1.0367	<0.0001
Ejection fraction (%)	0.94	0.9223–0.9503	<0.0001
E/e′ ratio	1.08	1.0596–1.0930	<0.0001
Septal wall thickness (mm)	1.18	1.1287–1.2238	<0.0001
LV mass index (g/m^2)	1.01	1.0096–1.0169	<0.0001
Pericardial effusion present*	2.95	2.0085–4.3281	<0.0001
MAPSE (cm)	0.10	0.0617–0.1603	<0.0001
LS (−%)	0.80	0.7608–0.8356	<0.0001
2D-RS (%)	0.97	0.9451–0.9852	<0.001
2D-CS (−%)	0.93	0.8985–0.9587	<0.0001
2D-GLS (−%)	0.77	0.7322–0.8054	<0.0001

*Dichotomous variable. †Glomerular filtration rate estimated with the MDRD formula. ‡Difference between pathologic and nonpathologic serologic free light chains.

LV = left ventricular; MAPSE = mitral annular plane systolic excursion; 2D-CS = mean two-dimensional circumferential peak negative strain; 2D-RS = mean two-dimensional radial peak positive strain; other abbreviations as in Tables 1 and 2.

To further describe those patients who were evaluated by echocardiography at the time of diagnosis before any first-line chemotherapy (i.e., chemotherapy naive), we performed the same analysis for this subgroup of patients (n = 113). Again, 2D-GLS (HR: 0.78, p < 0.0001) was still an independent predictor of survival in AL amyloidosis besides the difference of free light chains (HR: 1.0008, p = 0.005) and cTnT (HR: 2.78, p = 0.002) (Table 5).

In clinical routine, EF is one of the main parameters from echocardiography used for risk stratification in various cardiac diseases. We therefore investigated all patients with an LVEF ≥50% (n = 127). Interestingly, the Karnofsky index (HR: 0.95, p = 0.024) and 2D-GLS (HR: 0.86, p = 0.0018) were the only independent predictors of survival. cTnT and the difference of free light chains were no longer significant in this subgroup (Table 5). Similar results were found in the subgroup of patients with a reduced EF <50% (n = 71). Here, the Karnofsky index (HR: 0.94, p = 0.009), cTnT (HR: 2.21, p = 0.026), and 2D-GLS (HR: 0.86, p = 0.012) remained as independent predictors of survival (Online Table 2).

Including all subjects, the cutoff values discriminating survivors from nonsurvivors with the highest sensitivity and specificity were −10.65% for LS and −11.78% for 2D-GLS, respectively. For NT-proBNP and cTnT, the values were 3085 pg/ml and 0.01 μg/l, respectively. The corresponding Kaplan-Meier curves are presented in Figures 1A to 1D, and a more detailed description of the ROC analysis is shown in the Online Appendix and Online Figure S1.

We used different Cox models to further investigate the significance of LS and 2D-GLS for the prediction of outcome in AL amyloidosis. The addition of LS and 2D-GLS to a model, including baseline clinical variables and biomarkers, led to a significant increase in the power of the model. The model based on clinical variables (C: consisting of age, Karnofsky index, and NYHA class ≥2) with an overall chi-square (degree of freedom [df] = 3) of 80.27, was improved by log NT-proBNP (chi-square 41.97, df = 1, p < 0.001) and cTnT (chi-square 7.51, df = 1, p < 0.01), and further increased by LS (chi-square 16.81, df = 1, p < 0.001). Finally, 2D-GLS (chi-square 21.84, df = 1, p < 0.001) offered additional incremental information for the assessment of outcome (Fig. 3A, Table 6). In 2 further models, we assessed the value of EF in addition to the clinical model and in comparison to echocardiographic parameters (Figs. 3B and 3C, Table 6). These results were verified by the integrated discrimination improvement analysis. LV longitudinal strain (LS and 2D-GLS) yielded higher integrated discrimination improvement values compared with clinical variables, serological biomarkers, and echocardiographic parameters (Table 6).

Discussion

We reported on the largest, so far, cohort of consecutive patients with AL amyloidosis with systematic assessment of LV longitudinal function and its association with established risk parameters regarding prognosis.

The main findings of this study were: 1) NT-proBNP showed a strong correlation with parameters of longitudinal function (LS and 2D-GLS) in patients with AL amyloidosis; 2) the reduction of LS and 2D-GLS were both independently associated with prognosis in AL amyloidosis compared with standard echocardiographic parameters; 3) 2D-GLS and cTnT were independent predictors of survival in AL amyloidosis; and 4) LS and 2D-GLS provided incremental value to the combination of NT-proBNP, cTnT, and clinical parameters.

The poor outcome in patients with AL amyloidosis is mainly due to progressive cardiac dysfunction and limited treatment options for them. The main goal of therapy is to stop the production of amyloidogenic light chains, because this is associated with improvement of organ function (22), enhanced quality of life (23), and survival (24,25). However, in advanced cardiac disease, many patients cannot tolerate the side effects of any chemotherapy. Furthermore, new treatment strategies, including heart transplantation before high-dose chemotherapy and autologous stem cell support, require identification of patients at the highest risk of death (25). Thus, an early diagnosis of LV dysfunction with definition and classification of prognosis is crucial before any intervention.

The quantification of longitudinal function was considered to be a better measure of contractile myocardial function than only the geometric change of the left ventricle

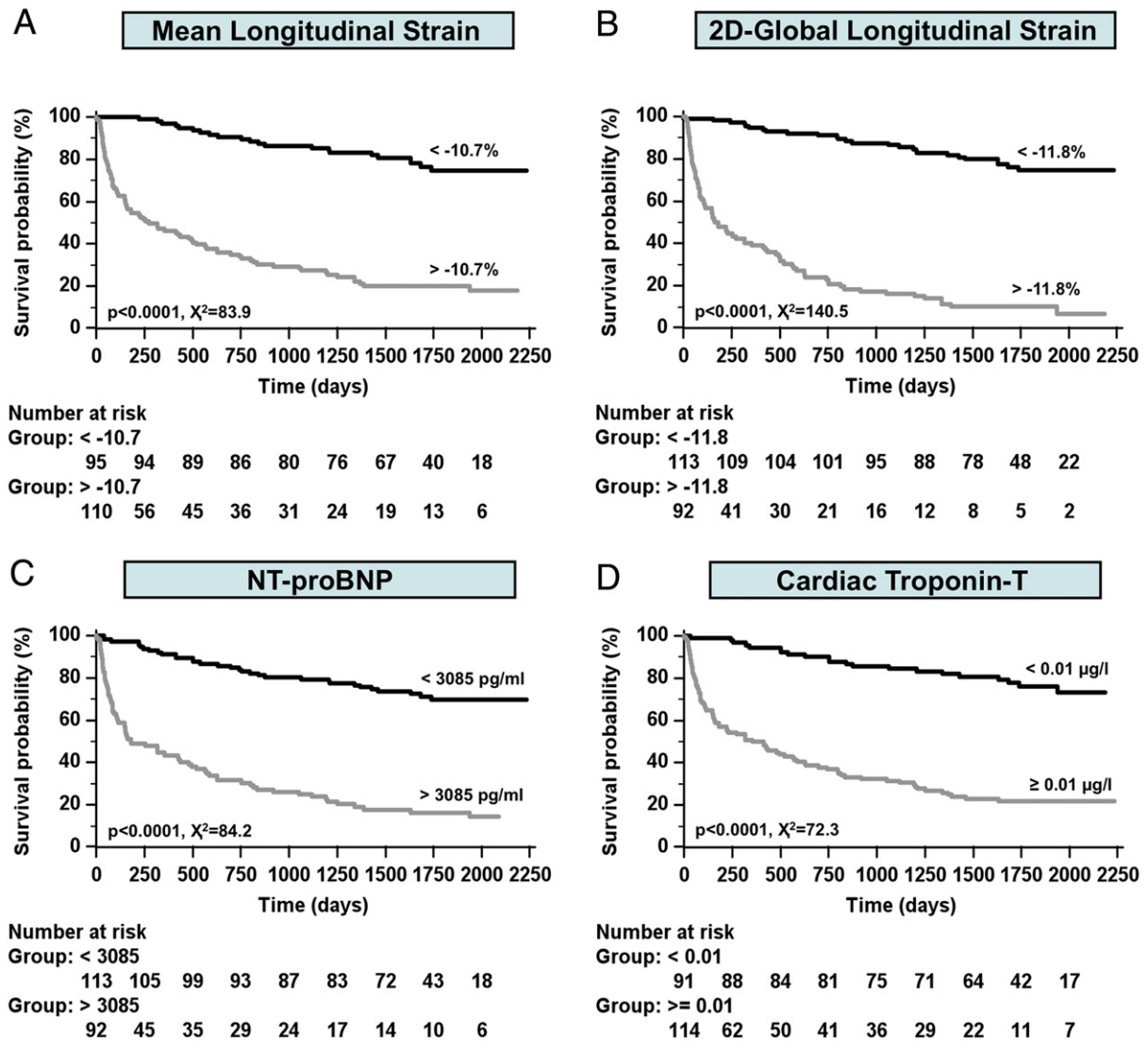

Figure 2 **Overall Survival in Patients With AL Amyloidosis**

Survival of patients with AL amyloidosis represented by Kaplan-Meier survival curves according to receiver-operator characteristic curve–derived cutoff values for **(A)** LS, **(B)** 2D-GLS, **(C)** N-terminal pro–B-type natriuretic peptide (NT-proBNP), and **(D)** cardiac troponin-T (cTnT). Time was determined as days from echocardiography. Abbreviations as in Figure 1.

estimated by calculating EF (26). The motion along the long axis of the heart is probably the most fundamental motion of the ventricles—twisting and untwisting in combination with longitudinal shortening (27). Longitudinal fibers are located in the subendocardium and subepicardium within a helical band as the underlying architecture of the heart (28). Given that histology, as well as magnetic resonance tomographic observations, demonstrated that the subendocardial myocardium is affected first by the disease (29) and, therefore, primarily longitudinal fibers are involved, this might partially explain the predominant prognostic implication of longitudinal function in the patients with preserved EF.

In congestive heart failure due to ischemic and nonischemic origin, the estimation of LV long-axis function by two-dimensional strain has emerged as an accurate predictor of all-cause mortality (18,19). This was in line with our results, because 2D-GLS still remained an independent predictor also in these subjects, despite a reduced EF. Also in aortic stenosis, LV longitudinal function was a measure of severity of cardiac impairment and degree of fibrosis, when the EF was still preserved (30–32). It was also demonstrated that in subclinical patients with cardiovascular risk factors, longitudinal function is impaired first (33). In contrast to a more heterogenous disease such as myocardial infarction, both longitudinal and circumferential deformations are independent risk factors for outcome and remodeling (34).

With the development of modern echocardiographic systems, the measurement of two-dimensional strain has

Table 4 Multivariable Proportional-Hazard Models

Echocardiographic Model (n = 205)	HR	95% CI	p Value
Left atrial volume index (ml/m^2)	0.9963	0.9807–1.0122	0.6471
Ejection fraction (%)	0.9926	0.9686–1.0171	0.5516
E/e′ ratio	1.0241	1.0018–1.0469	0.0349
Septal wall thickness (mm)	1.0579	0.9586–1.1675	0.2653
Left ventricular mass index (g/m^2)	0.9945	0.9865–1.0025	0.1766
Pericardial effusion present*	0.9713	0.6029–1.5646	0.9051
MAPSE (cm)	0.5994	0.2708–1.3270	0.2092
2D-GLS (−%)	0.8151	0.7604–0.8737	<0.0001

*Dichotomous variable.
Abbreviations as in Tables 2 and 3.

been proven to be reliable, angle independent, and more robust than TDI-derived strain, and can be calculated much easier and faster from standard two-dimensional grayscale images (35). Two-dimensional global longitudinal strain

Table 5 Comprehensive Clinical Models

Variable	HR	95% CI	p Value
Comprehensive model (n = 198)			
Age (yrs)	0.9978	0.9739–1.0223	0.8601
NYHA functional class (≥2)*	1.2316	0.7001–2.1663	0.4721
Karnofsky index (%)	0.9442	0.9161–0.9730	0.0002
MDRD (ml/min/1.73 m^2)	1.0011	0.9922–1.0101	0.8072
Free light chain difference (mg/l)	1.0002	1.0000–1.0003	0.0473
Log NT-proBNP (pg/ml)	1.0662	0.7006–1.6226	0.7658
cTnT (>0.03 μg/l)*	1.9666	1.2091–3.1987	0.0067
ECG low voltage present*	1.0302	0.6604–1.6072	0.8962
E/e′ ratio	1.0290	1.0067–1.0518	0.0109
2D-GLS (−%)	0.8511	0.7954–0.9106	<0.0001
Comprehensive model, chemotherapy naive patients (n = 113)			
Age (yrs)	1.0011	0.9738–1.0292	0.9382
NYHA functional class (≥2)*	1.1518	0.5512–2.4066	0.7084
Karnofsky index (%)	0.9682	0.9320–1.0058	0.0982
MDRD (ml/min/1.73 m^2)	0.9983	0.9854–1.0114	0.8031
Free light chain difference (mg/l)	1.0008	1.0002–1.0014	0.0051
Log NT-proBNP (pg/ml)	0.6789	0.3426–1.3452	0.2694
cTnT (>0.03 μg/l)*	2.7820	1.4633–5.2893	0.0019
ECG low voltage present*[a]	0.8893	0.5259–1.5039	0.6632
E/e′ ratio	1.0161	0.9894–1.0436	0.2424
2D-GLS (−%)	0.7825	0.7135–0.8581	<0.0001
Comprehensive model, EF ≥50% (n = 127)			
Age (yrs)	1.0149	0.9798–1.0513	0.4117
NYHA functional class (≥2)*	1.0176	0.5336–1.9403	0.9581
Karnofsky index (%)	0.9483	0.9058–0.9927	0.0236
MDRD (ml/min/1.73 m^2)	1.0013	0.9876–1.0152	0.8513
Free light chain difference (mg/l)	1.0005	0.9995–1.0016	0.3180
Log NT-proBNP (pg/ml)	1.0596	0.5542–2.0256	0.8618
cTnT (>0.03 μg/l)*	1.6893	0.7709–3.7017	0.1925
ECG low voltage present*	1.8030	0.9425–3.4493	0.0764
E/e′ ratio	1.0265	0.9838–1.0710	0.2306
2D-GLS (−%)	0.8590	0.7814–0.9444	0.0018

There are 5 missing NYHA muscular disorders due to polyneuropathy and 2 due to missing serologic free light chains. *Dichotomous variable.
Abbreviations as in Tables 1, 2, and 3.

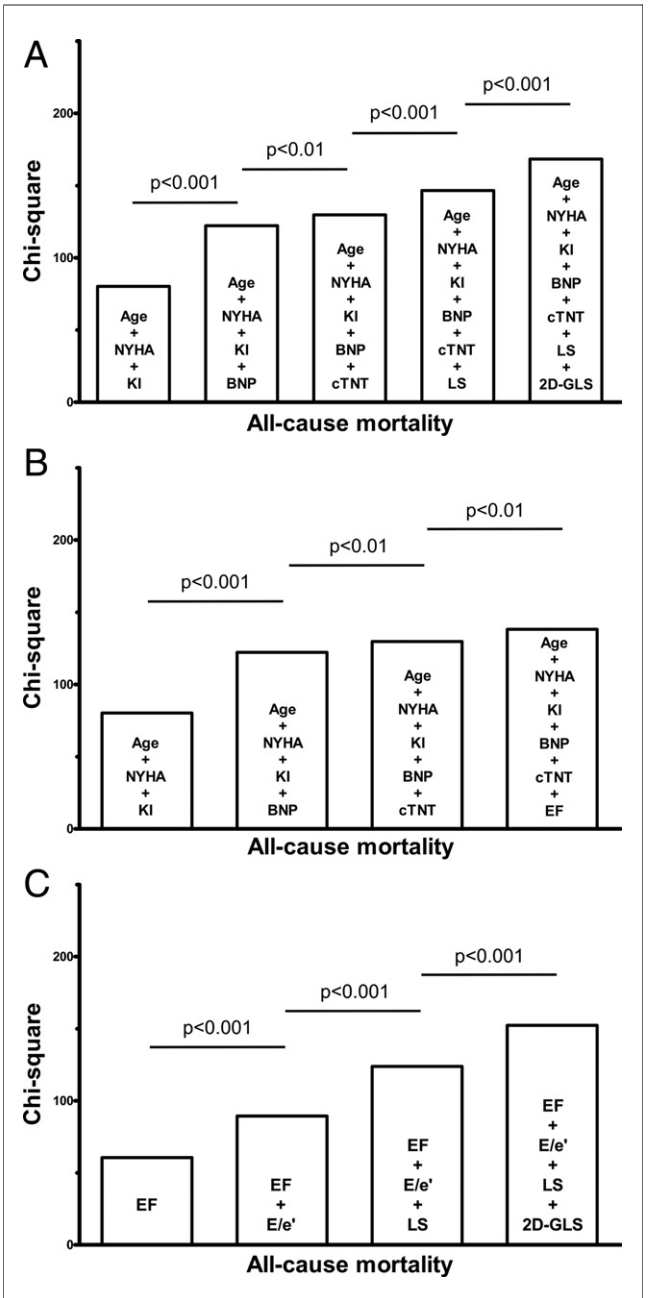

Figure 3 Incremental Predictive Value of LS and 2D-GLS in AL Amyloidosis

Three multivariate models were evaluated for the prediction of all-cause mortality in AL amyloidosis. In the first multivariate model, the clinical variables (age, Karnofsky index [KI] and New York Heart Association (NYHA) class ≥2) were entered together, followed by adding cTnT, log NT-proBNP, LS, and 2D-GLS. **(A)** LS and 2D-GLS offered incremental prognostic information to the model (Table 6). **(B)** In the second model (Table 6), the clinical risk factors (age, KI, and NYHA class ≥2) were entered together, followed by addition of cTnT, log NT-proBNP, and the ejection fraction (EF). The EF offered an incremental value to the clinical parameters and serological biomarkers. In the third model, only echocardiographic parameters were included. **(C)** When starting with the EF, followed by the E/e′ ratio and, finally, with the two parameters of left ventricular longitudinal function, LS and 2D-GLS, both offered incremental prognostic information (Table 6). Abbreviations as in Figure 1.

Table 6 Comparison of Multivariate Cox Regression Models

Model 1	Model 2	Chi-square Difference*	p Value	IDI
Comparison of multivariate Cox-regression models (n = 200)				
C	C + BNP	41.97	<0.001	0.086
C + BNP	C + BNP + cTnT	7.51	<0.01	0.011
C + BNP + cTnT	C + BNP + cTnT + LS	16.81	<0.001	0.027
C + BNP + cTnT +LS	C + BNP + cTnT + LS + 2D-GLS	21.84	<0.001	0.042
Clinical parameters and ejection fraction (n = 200)				
C	C + BNP	41.97	<0.001	0.086
C + BNP	C + BNP + cTnT	7.51	<0.01	0.011
C + BNP + cTnT	C + BNP + cTnT + EF	8.41	<0.01	0.005
Echocardiographic parameters (n = 205)				
EF	EF + E/e′	28.70	<0.001	0.059
EF + E/e′	EF + E/e′ + LS	34.36	<0.001	0.104
EF + E/e′ + LS	EF + E/e′ + LS + 2D-GLS	28.51	<0.001	0.057

C = Clinical model (age, NYHA class [dichotomous, cutoff ≥2], Karnofsky index); IDI = integrated discrimination improvement; other abbreviations as in Tables 1, 2, and 3.

measures the whole ventricle, including the apex, and not only the basal and midventricular segments, such as that in TDI-derived strain. With the use of two-dimensional Cardiac Performance Analysis, which is available for clinical routine, it is now possible to measure 2D-GLS with the same technique in studies recorded with different echocardiographic systems (36).

Systolic longitudinal strain and strain rate, as the current methods used to measure myocardial longitudinal function, seem to be more sensitive than myocardial systolic velocities measured with TDI to detect myocardial amyloid deposition in patients with AL amyloidosis, especially in subclinical disease (14,37). This notion is supported by other imaging methods such as cardiovascular magnetic resonance tomography, where the deposition of gadolinium, with a typical subendocardial enhancement, matches the distribution of amyloid-associated myocardial fibrosis (38). This deposition was independently associated with a poor prognosis (38–40). As mentioned previously, the longitudinal function in patients with AL amyloidosis using TDI-derived strain was reduced and also had an important prognostic relevance. Unfortunately, none of the previous studies comprehensively included all current echocardiographic and hematologic parameters, as well as biomarkers, in their analyses. According to previous studies, we also found an incremental prognostic value for LS measured with TDI. With two-dimensional strain, represented by 2D-GLS in this study, the subendocardial regions of the myocardium and the apex can now be evaluated in more detail, offering superior global strain information of the whole left ventricle. This may explain why the incremental value of 2D-GLS is incremental to LS in the sequential Cox regression models, as both represent a descriptor of LV longitudinal function. In addition, with this new method, it is also possible to measure radial and circumferential two-dimensional deformation parameters. Both are significantly reduced in AL amyloidosis and associated with poor survival in the univariate analysis; however, in our study population, they did not remain as independent predictors. Thus, evaluation of longitudinal function with two-dimensional deformation imaging might become the diagnostic method of choice to detect early longitudinal functional impairment and serve as a relevant echocardiographic "staging" parameter in patients with systemic AL amyloidosis.

In the present study, the largest serial investigation reported so far, the reduced LV longitudinal function was an independent predictor of survival in AL amyloidosis and offered incremental information beyond standard clinical and serological parameters. The data demonstrated that in patients with a reduced EF (<50%), but specifically in patients with AL amyloidosis and a preserved EF (≥50%), LV longitudinal function was one of the strongest prognostic tools that could be used, irrespective of previous therapies besides diastolic function, represented by the E/e′ ratio. This finding might be explained by the fact that the estimation of EF alone underestimated the severity of myocardial systolic dysfunction, especially in the setting of LV hypertrophy (41). In summary, these results underlined the great importance of both systolic and diastolic functional impairment in AL amyloidosis in concordance with independent predictors of survival, such as biomarkers.

NT-proBNP, cardiac troponins, and serum free AL are the currently recommended biomarkers for risk assessment in AL amyloidosis. The elevation of NT-proBNP in AL amyloidosis may reflect hormone production by cardiac myocytes as a result of compression by amyloid deposits (42). This suggests that elevated filling pressure is not the only determinant of an elevated NT-proBNP level in AL amyloidosis (43). Elevated levels of troponin and NT-proBNP were reported to be very good predictors of survival and are recommended for risk stratification in patients with AL amyloidosis (9,10,44). In our study, NT-proBNP, especially in contrast to cTnT, was highly correlated with LV longitudinal function. One could argue that NT-proBNP is a result of decreased longitudinal function and enhanced LV wall stress, whereas cTnT mainly represents myocardial damage. Thus, in the final multivariate analysis,

longitudinal function performed better than NT-proBNP. In accordance with previous studies, we confirmed that serum free ALs provided important prognostic information together with cTnT and 2D-GLS, especially in patients who were referred before any specific therapy for AL amyloidosis (45).

It is known that the level of cardiac biomarkers can be reduced if the applied chemotherapy has successfully eradicated the plasma clone in the bone marrow in AL amyloidosis (46). Furthermore, recent reports described the possibility of halting organ progression by using small molecules of tafamidis and diflunisal in TTR amyloidosis (47), eprodisate in AA amyloidosis (48), or reducing amyloid deposits by the SAP chelator CPHPC (49), as well as using the green tea polyphenol, epigallocatechin-3-gallate (50,51) in several forms of amyloidoses. Prospective clinical studies are needed to confirm these precursors or amyloid-directed effects and show whether the echocardiographic parameters analyzed in this study will also improve after successful therapy.

Conclusions

LV longitudinal function is significantly associated with cardiac biomarkers and increased mortality in AL amyloidosis. New echocardiographic parameters identified patients with the highest risk and served as independent predictors of survival. Quantification of LV longitudinal function by LS and 2D-GLS provided incremental prognostic value regarding cardiovascular outcome in AL amyloidosis and seemed to be superior to standard echocardiography and cardiac biomarkers. Thus, it might become the method of choice for the description of LV function in systemic AL amyloidosis. We therefore propose measurement of LV longitudinal function as a standard procedure for staging of patients with AL amyloidosis.

Acknowledgments

The authors thank their technicians, Anita Hager, Christiane Selter, and Arnold Siegmund, for their excellent assistance.

Reprint requests and correspondence: Dr. Stefan E. Hardt, Department of Cardiology, Angiology and Pneumology, University of Heidelberg, Im Neuenheimer Feld 410, 69120 Heidelberg, Germany. E-mail: stefan.hardt@med.uni-heidelberg.de.

REFERENCES

1. Gertz MA. Immunoglobulin light chain amyloidosis: 2011 update on diagnosis, risk-stratification, and management. Am J Hematol 2011; 86:180–6.
2. Falk RH, Comenzo RL, Skinner M. The systemic amyloidoses. N Engl J Med 1997;337:898–909.
3. Merlini G, Bellotti V. Molecular mechanisms of amyloidosis. N Engl J Med 2003;349:583–96.
4. Gertz MA, Greipp PR, Kyle RA. Classification of amyloidosis by the detection of clonal excess of plasma cells in the bone marrow. J Lab Clin Med 1991;118:33–9.
5. Sipe JD, Benson MD, Buxbaum JN, et al. Amyloid fibril protein nomenclature: 2010 recommendations from the nomenclature committee of the International Society of Amyloidosis. Amyloid 2010;17:101–4.
6. Selvanayagam JB, Hawkins PN, Paul B, Myerson SG, Neubauer S. Evaluation and management of the cardiac amyloidosis. J Am Coll Cardiol 2007;50:2101–10.
7. Kristen AV, Perz JB, Schonland SO, et al. Non-invasive predictors of survival in cardiac amyloidosis. Eur J Heart Fail 2007;9:617–24.
8. Dispenzieri A, Gertz MA, Kyle RA, et al. Serum cardiac troponins and N-terminal pro-brain natriuretic peptide: a staging system for primary systemic amyloidosis. J Clin Oncol 2004;22:3751–7.
9. Kristen AV, Giannitsis E, Lehrke S, et al. Assessment of disease severity and outcome in patients with systemic light-chain amyloidosis by the high-sensitivity troponin T assay. Blood 2010;116:2455–61.
10. Palladini G, Campana C, Klersy C, et al. Serum N-terminal pro-brain natriuretic peptide is a sensitive marker of myocardial dysfunction in AL amyloidosis. Circulation 2003;107:2440–5.
11. Gorcsan J III, Tanaka H. Echocardiographic assessment of myocardial strain. J Am Coll Cardiol 2011;58:1401–13.
12. Abraham TP, Dimaano VL, Liang HY. Role of tissue Doppler and strain echocardiography in current clinical practice. Circulation 2007; 116:2597–609.
13. Bellavia D, Abraham TP, Pellikka PA, et al. Detection of left ventricular systolic dysfunction in cardiac amyloidosis with strain rate echocardiography. J Am Soc Echocardiogr 2007;20:1194–202.
14. Bellavia D, Pellikka PA, Abraham TP, et al. Evidence of impaired left ventricular systolic function by Doppler myocardial imaging in patients with systemic amyloidosis and no evidence of cardiac involvement by standard two-dimensional and Doppler echocardiography. Am J Cardiol 2008;101:1039–45.
15. Koyama J, Ray-Sequin PA, Falk RH. Longitudinal myocardial function assessed by tissue velocity, strain, and strain rate tissue Doppler echocardiography in patients with AL (primary) cardiac amyloidosis. Circulation 2003;107:2446–52.
16. Bellavia D, Pellikka PA, AL-Zahrani GB, et al. Independent predictors of survival in primary systemic (AL) amyloidosis, including cardiac biomarkers and left ventricular strain imaging: an observational cohort study. J Am Soc Echocardiogr 2010;23:643–52.
17. Koyama J, Falk RH. Prognostic significance of strain Doppler imaging in light-chain amyloidosis. J Am Coll Cardiol Img 2010;3:333–42.
18. Stanton T, Leano R, Marwick TH. Prediction of all-cause mortality from global longitudinal speckle strain: comparison with ejection fraction and wall motion scoring. Circ Cardiovasc Imaging 2009;2:356–64.
19. Cho GY, Marwick TH, Kim HS, Kim MK, Hong KS, Oh DJ. Global 2-dimensional strain as a new prognosticator in patients with heart failure. J Am Coll Cardiol 2009;54:618–24.
20. Buss SJ, Wolf D, Korosoglou G, et al. Myocardial left ventricular dysfunction in patients with systemic lupus erythematosus: new insights from tissue Doppler and strain imaging. J Rheumatol 2010;37:79–86.
21. Pencina MJ, D'Agostino RB Sr., D'Agostino RB Jr., Vasan RS. Evaluating the added predictive ability of a new marker: from area under the ROC curve to reclassification and beyond. Stat Med 2008;27:157–72; discussion 207–12.
22. Dispenzieri A, Lacy MQ, Katzmann JA, et al. Absolute values of immunoglobulin free light chains are prognostic in patients with primary systemic amyloidosis undergoing peripheral blood stem cell transplantation. Blood 2006;107:3378–83.
23. Seldin DC, Anderson JJ, Sanchorawala V, et al. Improvement in quality of life of patients with AL amyloidosis treated with high-dose melphalan and autologous stem cell transplantation. Blood 2004;104:1888–93.
24. Skinner M, Sanchorawala V, Seldin DC, et al. High-dose melphalan and autologous stem-cell transplantation in patients with AL amyloidosis: an 8-year study. Ann Intern Med 2004;140:85–93.
25. Kristen AV, Sack FU, Schonland SO, et al. Staged heart transplantation and chemotherapy as a treatment option in patients with severe cardiac light-chain amyloidosis. Eur J Heart Fail 2009;11:1014–20.
26. Dumesnil JG, Shoucri RM, Laurenceau JL, Turcot J. A mathematical model of the dynamic geometry of the intact left ventricle and its application to clinical data. Circulation 1979;59:1024–34.
27. Carlsson M, Ugander M, Mosen H, Buhre T, Arheden H. Atrioventricular plane displacement is the major contributor to left ventricular pumping in healthy adults, athletes, and patients with dilated cardiomyopathy. Am J Physiol Heart Circ Physiol 2007;292: H1452–9.

28. Kocica MJ, Corno AF, Carreras-Costa F, et al. The helical ventricular myocardial band: global, three-dimensional, functional architecture of the ventricular myocardium. Eur J Cardiothorac Surg 2006;29(Suppl 1):S21–40.
29. Vogelsberg H, Mahrholdt H, Deluigi CC, et al. Cardiovascular magnetic resonance in clinically suspected cardiac amyloidosis: noninvasive imaging compared to endomyocardial biopsy. J Am Coll Cardiol 2008;51:1022–30.
30. Pibarot P, Dumesnil JG. Longitudinal myocardial shortening in aortic stenosis: ready for prime time after 30 years of research? Heart 2009;96:95–6.
31. Herrmann S, Stork S, Niemann M, et al. Low-gradient aortic valve stenosis myocardial fibrosis and its influence on function and outcome. J Am Coll Cardiol 2011;58:402–12.
32. Pibarot P, Dumesnil JG. Paradoxical low-flow, low-gradient aortic stenosis adding new pieces to the puzzle. J Am Coll Cardiol 2011;58:413–5.
33. Mizuguchi Y, Oishi Y, Miyoshi H, Iuchi A, Nagase N, Oki T. The functional role of longitudinal, circumferential, and radial myocardial deformation for regulating the early impairment of left ventricular contraction and relaxation in patients with cardiovascular risk factors: a study with two-dimensional strain imaging. J Am Soc Echocardiogr 2008;21:1138–44.
34. Hung CL, Verma A, Uno H, et al. Longitudinal and circumferential strain rate, left ventricular remodeling, and prognosis after myocardial infarction. J Am Coll Cardiol 2010;56:1812–22.
35. Geyer H, Caracciolo G, Abe H, et al. Assessment of myocardial mechanics using speckle tracking echocardiography: fundamentals and clinical applications. J Am Soc Echocardiogr 2010;23:351–69; quiz 453–5.
36. Koopman LP, Slorach C, Manlhiot C, et al. Assessment of myocardial deformation in children using Digital Imaging and Communications in Medicine (DICOM) data and vendor independent speckle tracking software. J Am Soc Echocardiogr 2011;24:37–44.
37. Buss SJ, Mereles D, Emami M, et al. Rapid assessment of longitudinal systolic left ventricular function using speckle tracking of the mitral annulus. Clin Res Cardiol 2012;101:273–80.
38. Hosch W, Kristen AV, Libicher M, et al. Late enhancement in cardiac amyloidosis: correlation of MRI enhancement pattern with histopathological findings. Amyloid 2008;15:196–204.
39. Lehrke S, Steen H, Kristen AV, et al. Serum levels of NT-proBNP as surrogate for cardiac amyloid burden: new evidence from gadolinium-enhanced cardiac magnetic resonance imaging in patients with amyloidosis. Amyloid 2009;16:187–95.
40. Austin BA, Tang WH, Rodriguez ER, et al. Delayed hyper-enhancement magnetic resonance imaging provides incremental diagnostic and prognostic utility in suspected cardiac amyloidosis. J Am Coll Cardiol Img 2009;2:1369–77.
41. Cramariuc D, Cioffi G, Rieck AE, et al. Low-flow aortic stenosis in asymptomatic patients: valvular-arterial impedance and systolic function from the SEAS Substudy. J Am Coll Cardiol Img 2009;2:390–9.
42. Takemura G, Takatsu Y, Doyama K, et al. Expression of atrial and brain natriuretic peptides and their genes in hearts of patients with cardiac amyloidosis. J Am Coll Cardiol 1998;31:754–65.
43. Nordlinger M, Magnani B, Skinner M, Falk RH. Is elevated plasma B-natriuretic peptide in amyloidosis simply a function of the presence of heart failure? Am J Cardiol 2005;96:982–4.
44. Dispenzieri A, Gertz MA, Kyle RA, et al. Prognostication of survival using cardiac troponins and N-terminal pro-brain natriuretic peptide in patients with primary systemic amyloidosis undergoing peripheral blood stem cell transplantation. Blood 2004;104:1881–7.
45. Bochtler T, Hegenbart U, Heiss C, et al. Evaluation of the serum-free light chain test in untreated patients with AL amyloidosis. Haematologica 2008;93:459–62.
46. Dietrich S, Schonland SO, Benner A, et al. Treatment with intravenous melphalan and dexamethasone is not able to overcome the poor prognosis of patients with newly diagnosed systemic light chain amyloidosis and severe cardiac involvement. Blood 2010;116:522–8.
47. Coelho T, Maia LF, da Silva Martins A, et al. Tafamidis for transthyretin familial amyloid polyneuropathy: A randomized, controlled trial. Neurology 2012;79:785–92.
48. Dember LM, Hawkins PN, Hazenberg BP, et al. Eprodisate for the treatment of renal disease in AA amyloidosis. N Engl J Med 2007;356:2349–60.
49. Gillmore JD, Tennent GA, Hutchinson WL, et al. Sustained pharmacological depletion of serum amyloid P component in patients with systemic amyloidosis. Br J Haematol 2010;148:760–7.
50. Miyata M, Sato T, Kugimiya M, et al. The crystal structure of the green tea polyphenol (−)-epigallocatechin gallate-transthyretin complex reveals a novel binding site distinct from the thyroxine binding site. Biochemistry 2010;49:6104–14.
51. Mereles D, Buss SJ, Hardt SE, Hunstein W, Katus HA. Effects of the main green tea polyphenol epigallocatechin-3-gallate on cardiac involvement in patients with AL amyloidosis. Clin Res Cardiol 2010;99:483–90.

Key Words: amyloidosis ■ biomarker ■ echocardiography ■ left ventricular function ■ prognosis ■ tissue Doppler ■ two-dimensional strain imaging.

APPENDIX

For supplemental data, tables, and videos, please see the online version of this article.